Sequential MCMC for Signal Recovery of Multiple Nonstationary Targets Using an Array of Sensors

William Ng, James P. Reilly*, Thia Kirubarajan, and Jean-René Larocque
Department of Electrical and Computer Engineering,
McMaster University, 1280 Main St. W.,
Hamilton, Ontario,
Canada L8S 4K1

Abstract

This paper proposes a new alternative to beamforming for extraction of multiple waveforms of desired sources in the presence of interfering signals. Waveform extraction is useful for communications in hostile environments and to aid in classification of targets in radar applications.

Conventional approaches to this problem use a sequence of disjoint procedures for waveform extraction. These include model order detection, direction of arrival (DOA) estimation, DOA tracking, and then finally beamforming. In contrast, the proposed approach combines all these processes jointly. A disctinct advantage of the proposed method is the fact that it is effective in highly nonstationary environments, where classical beamforming approaches fail. Unlike modern competing methods, like the LPA-beamformer [1] [2], the proposed method is not model sensitive, and does not assume smooth DOA motion within an observation window.

The proposed method is based sequential Monte Carlo (otherwise known as *particle filtering*) techniques for estimation and tracking of the required DOAs. Once the DOA estimates are available, the desired source waveforms can be extracted using a *maximum a posteriori* (MAP) procedure. Model order detection is obtained using a reversible jump Markov chain Monte Carlo (RJMCMC) resampling algorithm. Simulation results, which compare performance to the extended Kalman filter and the LPA beamformer, are presented.

I. Introduction

The problem of recovering waveforms from multiple sources is of considerable interest in electronic systems. This problem has application in communications in hostile environments, or in radar where the waveforms from the multiple targets are to be used to aid in target classification. Standard approaches to this problem rely on arrays of sensors; first, the number of sources or targets are detected (this is otherwise known as order detection), then the corresponding directions-of-arrival (DOAs) are estimated, and then tracked. Once smoothed of filtered DOA estimates are available, the desired waveforms can then be recovered using beamforming techniques. In this paper we concentrate specifically on the more difficult case where the sources

Permission to publish abstract separately is granted.
J. Reilly, corresponding author: ph: 905 525 9140 x22895, fax: 905 521 2922, email: reillyj@mcmaster.ca

are highly mobile or nonstationary in angle. In the following portion of this Introduction, we briefly discuss the shortcomings of the order detection, the DOA estimation, the tracking, and the beamforming components as they relate to the waveform extraction problem.

As we see later, for signal recovery to perform well, the DOAs must be properly estimated and tracked. Current DOA estimation techniques (MUSIC [3], ML [4], WSF, [5] etc) do not behave well in the nonstationary case since these methods depend on covariance matrices averaged over several past observations. Thus, the environment must be homogeneous and stationary over the observation window, and performance degrades when these conditions are violated. An analogous situation holds with respect to conventional order detection methods (e.g., the AIC and MDL criteria [6]).

Conventionally, in DOA tracking applications, the DOA estimation phase precedes the tracking process as a completely disjoint operation. That is, signal processing precedes state estimation. In particular, tracking using DOA-only measurements, which has been considered extensively in the literature (see [7], [8], [9], [10]), is a challenging problem because of nonlinearity and observability problems.

In the case where the DOAs are nonstationary, DOA estimation and tracking can be approached using *state-space models*. The aim is to estimate the state process using the observations that update the posterior distribution of interest as new observations arrive. Classical methods to obtain approximations to the desired distributions include analytical approximations, such as the extended Kalman filter [11], the Gaussian sum filter [12], and deterministic numerical integration techniques [13]. The extended Kalman filter (EKF) and Gaussian sum filter are computationally cheap, but fail or diverge in some difficult scenarios. In particular, if the nonlinearities in the state and measurement equations are significant, then the EKF's performance is degraded [14].

Beamforming [15] [16], a form of spatial filtering, is regarded as the ability of an array to capture signals incident from a particular direction. The objective of beamforming is to estimate a desired signal waveform arriving from a known direction, in the presence of noise and interfering signals, or to separate desired signals incident from different spatial locations or directions. The extracted signals can then be used as signatures or features for classification among different objects or targets in radar and sonar applications. Beamforming has also proven very successful in communications in hostile environments.

Typical beamforming approaches were developed assuming one desired source and considering other sources as interference. To protect the desired source and to suppress the others, precise knowledge of the desired source DOA must be available. Methods like MVDR, GSC, [15] etc., are just a few examples that require these assumptions to be valid for reasonable performance. Thus these algorithms could only find application in the case where the signal sources or targets are *stationary* and where their positions are perfectly known throughout the entire engagement. Unfortunately, in practical systems and scenarios these assumptions are easily violated: the target source may move from observation to observation and the assumed DOAs may be different from the actual ones, and the number of sources may not be known, resulting in degraded

performance in signal extraction. As a result, in applications where the sources are mobile, traditional beamforming techniques are not very precise and better techniques are needed.

Recently, beamforming methods have been developed to handle nonstationary sources [1] [2] [17]. These methods propose the use of a polynomial model to estimate DOA motion within a short observation period (window) so that beamforming is possible in mildly nonstationary environments. With these methods, the angular velocities of the DOA motion is taken into account, and optimization techniques are then used to search for the optimal DOAs of the sources. Once the estimates are available, traditional beamforming algorithms could then be used to extract signals of interest. While these methods take target motion into account, they still do not address the critical model order selection problem; also, the performance relies heavily on the smoothness of target motion within the observation period. The PASTd approach [18] has also been proposed as a means of dealing with nonstationary targets. This method estimates a noise subspace over a sliding window from the observed data. Then, from this subspace, the number of sources can be determined and the DOAs tracked. Thus, assumptions about stationary sources and the knowledge of the number of sources is relaxed with this approach. However, The PASTd method assumes that the subspace is constant within the window, which means the DOAs must be almost stationary. Thus the method fails to track and extract the sources if they move substantially within the window.

The performance of standard beamforming algorithms is sensitive to error in the DOA estimate of the target, and deteriorates very significantly if the estimated DOA is different from the true one. Robustness to DOA uncertainty [1] has been introduced such that the main lobe width is traded off with the degradation caused by the deviation of the estimated and true DOAs.

In this paper, we present a novel alternative method to beamforming for online recovery of an unknown number of desired source waveforms in the presence of interference, that is effective in nonstationary conditions. The proposed method performs the DOA estimation/tracking, and the order detection components of the waveform extraction problem jointly in one seamless operation, rather than disjointly as before. The proposed method uses the sequential MC (Monte Carlo) methods in conjunction with the MCMC (Markov Chain Monte Carlo) methods [19] [20], that have emerged as useful methods in the signal processing arena. They are Bayesian methods based on the idea of numerically sampling posterior distributions of interest that are difficult or impossible to handle analytically. Using the histogram so obtained from these samples, statistical inferences on parameters of interest can be made. The sequential MC methods (also known as *particle filters*) [19], [21], [22] are suitable for estimating the state process using the observations and hence recursively updating the posterior distribution of interest as new observations arrive. Model order detection is achieved using the reversible jump MCMC procedure [23]. Simulation results show that the proposed particle filtering approach for waveform recovery does not suffer from the drawbacks associated with the more standard approaches, as discussed above, at addressing this problem.

The proposed procedure is first to determine the number of incident signals, and then estimate their respective DOAs using sequential Monte Carlo methods. We then use the estimated DOAs

to extract the desired source amplitudes using a *maximum a posteriori* (MAP) procedure. The desired sources can be distinguished from interferences using a priori knowledge of the desired source waveforms.

This paper is organized as follows. Section 2 presents the state-space signal model and the derivation of the necessary distributions. Section 3 describes the derivation of the sequential update of the target posterior distribution. Section 4 describes the reversible jump MCMC procedure that facilitates model order detection. Section 5 presents simulation results and compares the proposed method with the EKF [24] [14] and the LPA-beamformer [1] [2]. Conclusions are given in Section 6.

Notation: Bold upper case symbols denote matrices, bold lower case symbols denote vectors. The superscript ^{H} denotes the transpose operation, and the symbol "$\sim$" means "distributed as." The quantity $p(\cdot)$ denotes a prior probability distribution, $l(\cdot)$ denotes a likelihood function, and $\pi(\cdot)$ denotes a posterior distribution. The quantity $\mathcal{N}(\mu, \sigma^2)$ indicates a real normal distribution with mean μ and variance σ^2. The symbol $\mathcal{N}_c(\cdot, \cdot)$ denotes the corresponding complex normal distribution. The quantity $\mathcal{U}(a, b)$ indicates a uniform distribution over the interval $[a, b]$.

II. The State-Space Model

A. The State-Space Model

The transmission medium is assumed to be isotropic and nondispersive so that the radiation propagates along straight lines, and the sources are assumed *narrowband* and in the *far-field* of the array. In other words, the radiation impinging on the array is in the form of a sum of plane waves.

We denote the number of narrowband plane waves impinging on an M-element array from distinct directions at time t as $k(t)$, which is unknown and time–varying, such that $k(t) < M$ for all t. The signals are assumed to have the same known center frequency and, hence, the effect of a time delay on the received waveforms is simply a phase shift. Denoting the DOA vector by $\boldsymbol{\phi}(t) \in [0, 2\pi]^{k(t)}$, we define the steering matrix by $\boldsymbol{S}(\boldsymbol{\phi}(t)) \in \mathcal{C}^{M \times k(t)}$ as follows:

$$\boldsymbol{S}(\boldsymbol{\phi}(t)) \quad = \quad [\boldsymbol{s}(\phi_1(t)), \boldsymbol{s}(\phi_2(t)), \ldots, \boldsymbol{s}(\phi_k(t))], \tag{1}$$

where $k = 1, 2, ..., k(t)$. Each column of $\boldsymbol{S}(\boldsymbol{\phi}(t))$ is the steering vector corresponding to a particular source, defined as follows:

$$\boldsymbol{s}(\phi_k(t)) \quad = \quad [e^{-jd_1\xi_k(t)}, e^{-jd_2\xi_k(t)}, \ldots, e^{-jd_M\xi_k}]^T, \tag{2}$$

where

$$\xi_k(t) = (2\pi/\lambda) \sin \phi_k(t). \tag{3}$$

The quantity $\phi_k(t)$ is the angle of the kth source incident onto the array at time t, d_m for $m = 1, 2, \ldots, M$ is the position of the mth sensor, and λ is the wavelength. Denote a complex vector of observations $\boldsymbol{y}(t) \in \mathcal{C}^M$ that represents the data received by a linear array of sensors

at the tth snapshot, and a complex vector of amplitudes of the sources at the tth instant by $\boldsymbol{a}(t) \in \mathcal{C}^{k(t)}$. We adopt a first order state-space Markov model in the proposed sequential sampling approach. It is assumed that the states $[\boldsymbol{\phi}(t), \boldsymbol{a}(t)]$ evolve according to the following equations:

$$\begin{aligned} \boldsymbol{\phi}(t) &= \boldsymbol{\phi}(t-1) + \sigma_w \boldsymbol{w}(t), & (4) \\ \boldsymbol{a}(t) &\sim \mathcal{N}(\boldsymbol{0}, \delta^2 \sigma_w^2 \left[\boldsymbol{S}^H(\boldsymbol{\phi}(t))\boldsymbol{S}(\boldsymbol{\phi}(t))\right]^{-1}), & (5) \end{aligned}$$

whereas the observation equation is defined as:

$$\boldsymbol{y}(t) = \boldsymbol{S}(\boldsymbol{\phi}(t))\boldsymbol{a}(t) + \sigma_n \boldsymbol{v}(t), \quad (6)$$

where the noise variables $\boldsymbol{v}(t) \in \mathcal{C}^M$ and $\boldsymbol{w}(t) \in \mathcal{R}^{k(t)}$ are Gaussian variables with zero mean and unit variance uncorrelated with the signal and each other, the noise variances σ_w and σ_v are assumed unknown and constant (for a stationary system), and the hyperparameter δ^2 is set to an a priori estimate of the SNR[25].

We define the vector $\boldsymbol{\theta}_{1:t}$ of unknown parameters as follows:

$$\boldsymbol{\theta}_{1:t} \triangleq (\{\boldsymbol{\phi}_{k(t)}\}_{1:t}, \{\boldsymbol{a}_{k(t)}\}_{1:t}, k_{1:t}, \sigma_v^2, \sigma_w^2), \quad (7)$$

where the notation $(\cdot)_{t_1:t_2}$ denotes all values of the argument from time t_1 to t_2. Using Bayes' theorem, we have the following expression for the joint posterior distribution $\pi(\boldsymbol{\theta}_{1:t})$ from time 1 to t, involving the likelihood function $l(\boldsymbol{y}_{1:t}|\boldsymbol{\theta}_{1:t})$ and the joint prior distribution $p(\boldsymbol{\theta}_{1:t})$:

$$\pi(\boldsymbol{\theta}_{1:t}) \propto l(\boldsymbol{y}_{1:t}|\boldsymbol{\theta}_{1:t}) p(\boldsymbol{\theta}_{1:t}). \quad (8)$$

The above can be expanded to give

$$\pi(\boldsymbol{\theta}_{1:t}) \propto l(\boldsymbol{y}_{1:t}|\boldsymbol{\phi}_{1:t}, \boldsymbol{a}_{1:t}, k_{1:t}, \sigma_v^2, \sigma_w^2) p(\boldsymbol{\phi}_{1:t}|k_{1:t}, \sigma_v^2) p(\boldsymbol{a}_{1:t}|\boldsymbol{\phi}_{1:t}, k_{1:t}, \sigma_w^2) p(\sigma_v^2) p(\sigma_w^2) p(k_{1:t}). \quad (9)$$

The quantity δ^2 in (9) is a hyperparameter equivalent to the inverse signal to noise ratio. Assuming the observations, given the states are *iid*, the conditional update likelihoods of the states are also *iid*, and the distribution of the initial states is uniform, we can express the following individual distributions, using the Markov properties of the model, as follows:

$$\begin{aligned} l(\boldsymbol{y}_{1:t}|\boldsymbol{\phi}_{1:t}, \boldsymbol{a}_{1:t}, k_{1:t}, \sigma_v^2, \sigma_w^2) &= \prod_{l=1}^{t} \mathcal{N}(\boldsymbol{S}(\boldsymbol{\phi}_l)\boldsymbol{a}_l, \sigma_w^2 \boldsymbol{I}_M), & (10) \\ p(\boldsymbol{\phi}_{1:t}|k_{1:t}, \sigma_v^2) &= \prod_{l=1}^{t} \mathcal{N}(\boldsymbol{\phi}_{l-1}, \sigma_v^2 \boldsymbol{I}_{k_l}), & (11) \\ p(\boldsymbol{a}_{1:t}|\boldsymbol{\phi}_{1:t}, k_{1:t}, \sigma_w^2) &= \prod_{l=1}^{t} \mathcal{N}(\boldsymbol{0}, \delta^2 \sigma_w^2 \left[\boldsymbol{S}^H(\boldsymbol{\phi}_l)\boldsymbol{S}(\boldsymbol{\phi}_l)\right]^{-1}). & (12) \end{aligned}$$

The prior distribution for the model order k is assigned a discrete uniform distribution equal to $\Lambda = 1/k_{\max}, k = 0, \ldots, k_{\max}$, where $k_{\max}$ is the maximum allowable model order, equal to

$M-1$. The prior distributions of the noise variances are both assumed to follow the inverse Gamma distribution, which is the conjugate distribution for the Normal distribution as follows:

$$p(\sigma_v^2) \sim \mathcal{IG}(\frac{\alpha_0}{2}, \frac{\gamma_0}{2}), \tag{13}$$

$$p(\sigma_w^2) \sim \mathcal{IG}(\alpha_1, \gamma_1), \tag{14}$$

where $\alpha_0, \alpha_1, \gamma_0, \gamma_1$ are hyperparameters.

Substituting (10) - (14) into (9) and rearranging, it can be shown [25][26] that the posterior distribution $\pi(\boldsymbol{\theta}_{1:t})$ can be represented as follows:

$$\begin{aligned}\pi(\boldsymbol{\theta}_{1:t}) \propto & \prod_{l=1}^{t} \frac{1}{\sigma_w^{2k_l}\pi^{k_l}} \exp\left[\frac{-1}{\sigma_w^2}(\boldsymbol{a}_l - \boldsymbol{m}_{\boldsymbol{a}_l})^H \boldsymbol{\Sigma}_{\boldsymbol{a}_l}^{-1}(\boldsymbol{a}_l - \boldsymbol{m}_{\boldsymbol{a}_l})\right] \\ & \times \prod_{l=1}^{t} \frac{1}{\sigma_w^{2M}\delta^{2k_l}} \exp\left[\frac{-1}{\sigma_w^2}\boldsymbol{y}_l^H \boldsymbol{P}_S^{\perp}(\boldsymbol{\phi}_l)\boldsymbol{y}_l\right] \\ & \times \prod_{l=1}^{t} \frac{|\boldsymbol{S}^H(\boldsymbol{\phi}_l)\boldsymbol{S}(\boldsymbol{\phi}_l)|}{\sigma_v^{2k_l/2}(2\pi)^{k_l/2}} \exp\left[\frac{-1}{2\sigma_v^2}(\boldsymbol{\phi}_l - \boldsymbol{\phi}_{l-1})^H(\boldsymbol{\phi}_l - \boldsymbol{\phi}_{l-1})\right] \\ & \times \sigma_v^{2(-\frac{\alpha_0}{2}-1)} \exp\left[\frac{-\gamma_0}{2\sigma_v^2}\right] \times \sigma_w^{2(-\alpha_1-1)} \exp\left[\frac{-\gamma_1}{\sigma_w^2}\right] \times \prod_{l=1}^{t} \Lambda,\end{aligned} \tag{15}$$

where

$$\boldsymbol{\Sigma}_{\boldsymbol{a}_l}^{-1} = \boldsymbol{S}^H(\boldsymbol{\phi}_l)\boldsymbol{S}(\boldsymbol{\phi}_l)(1 + 1/\delta^2), \tag{16}$$

$$\boldsymbol{m}_{\boldsymbol{a}_l} = \boldsymbol{\Sigma}_{\boldsymbol{a}_l}\boldsymbol{S}^H(\boldsymbol{\phi}_l)\boldsymbol{y}_l, \tag{17}$$

and

$$\boldsymbol{P}_S^{\perp}(\boldsymbol{\phi}_l) = \boldsymbol{I} - \frac{\boldsymbol{S}(\boldsymbol{\phi}_l)[\boldsymbol{S}^H(\boldsymbol{\phi}_l)\boldsymbol{S}(\boldsymbol{\phi}_l)]^{-1}\boldsymbol{S}^H(\boldsymbol{\phi}_l)\boldsymbol{y}_l}{(1 + 1/\delta^2)}. \tag{18}$$

From (15), it is seen that (17) is a *maximum a posteriori* (MAP) estimate of the amplitudes $\boldsymbol{a}_l$, which implies that the amplitudes need not be included in the particle filter but can be estimated at each iteration after the sampling of the other parameters. Finally, integrating out $\boldsymbol{a}_l$ analytically from (15) yields

$$\begin{aligned}\pi(\boldsymbol{\alpha}_{1:t}) \propto & \prod_{l=1}^{t} \frac{1}{\sigma_w^{2M}(1+\delta^2)^{k_l}} \exp\left[\frac{-1}{\sigma_w^2}\boldsymbol{y}_l^H \boldsymbol{P}_S^{\perp}(\boldsymbol{\phi}_l)\boldsymbol{y}_l\right] \\ & \times \prod_{l=1}^{t} \frac{1}{\sigma_v^{2k_l/2}(2\pi)^{k_l/2}} \exp\left[\frac{-1}{2\sigma_v^2}(\boldsymbol{\phi}_l - \boldsymbol{\phi}_{l-1})^H(\boldsymbol{\phi}_l - \boldsymbol{\phi}_{l-1})\right] \\ & \times \sigma_v^{2(-\frac{\alpha_0}{2}-1)} \exp\left[\frac{-\gamma_0}{2\sigma_v^2}\right] \times \sigma_w^{2(-\alpha_1-1)} \exp\left[\frac{-\gamma_1}{\sigma_w^2}\right] \times \prod_{l=1}^{t} \Lambda,\end{aligned} \tag{19}$$

where the prior on the model order has been absorbed into the constant of proportionality. The above yields a much simpler posterior distribution in terms of the remaining parameters. As a result, we can write the parameter vector $\boldsymbol{\alpha}_{1:t}$ as follows:

$$\boldsymbol{\alpha}_{1:t} \triangleq (\boldsymbol{\phi}_{1:t}, k_{1:t}, \sigma_v^2, \sigma_w^2). \tag{20}$$

It is also possible to obtain the MAP estimators of the variance parameters as follows:

$$\sigma^2_{v,MAP} = \frac{\frac{\gamma_0}{2} + \frac{1}{2}\sum_{l=1}^{t}\left(\boldsymbol{\phi}_l - \boldsymbol{\phi}_{l-1}\right)^H\left(\boldsymbol{\phi}_l - \boldsymbol{\phi}_{l-1}\right)}{\frac{\nu_0}{2} + \frac{1}{2}\sum_{l=1}^{t}k(l) + 1}, \tag{21}$$

$$\sigma^2_{v,MAP} = \frac{\gamma_1 + \sum_{l=1}^{t}\boldsymbol{y}_l^H\boldsymbol{P}_S^{\perp}(\boldsymbol{\phi}_l)\boldsymbol{y}_l}{\nu_1 + Mt + 1}. \tag{22}$$

Thus, the proposed approach is to use the posterior distribution of (19) to estimate the DOAs $\boldsymbol{\phi}(t)$, and the model order $k(t)$, as discussed later. Once these estimates are available, the objective of this work can be achieved, which is to estimate the desired signal amplitudes. This is done using (17).

III. Sequential MC (SMC)

A. Bayesian Importance Sampling

Monte Carlo sampling methods can be used to generate a numerical approximation in the form of a histogram corresponding to an arbitrary distribution of interest. To illustrate the use of this approach, consider a function $f(\boldsymbol{x})$ of $\boldsymbol{x}$. The expected value of the function over a probability distribution function $\pi(\boldsymbol{x})$ can be defined as:

$$I_f = E_{\pi(\boldsymbol{x})}(f(\boldsymbol{x})) = \int \pi(\boldsymbol{x})f(\boldsymbol{x})d\boldsymbol{x}. \tag{23}$$

This expectation may be difficult or impossible to evaluate analytically. However, let's assume that we are able to draw N *iid* samples $\{\boldsymbol{x}^{(i)}; i = 1, 2, \ldots, N\}$ from the desired distribution $\pi(\boldsymbol{x})$. We can then numerically approximate this distribution as:

$$\hat{\pi}_N(d\boldsymbol{x}) = \frac{1}{N}\sum_{i=1}^{N}\delta_{\boldsymbol{x}^{(i)}}d\boldsymbol{x}, \tag{24}$$

where $d\boldsymbol{x}$ is a small, finite region surrounding an $\boldsymbol{x}$ of interest and $\delta_{\boldsymbol{x}^{(i)}}$ is an indicator function defined as:

$$\delta_{\boldsymbol{x}^{(i)}}(d\boldsymbol{x}) = \begin{cases} 1, & \text{if } \boldsymbol{x}^{(i)} \in d\boldsymbol{x}, \\ 0, & \text{otherwise.} \end{cases} \tag{25}$$

As a result, we can approximate the expected value of $f(\boldsymbol{x})$ as follows:

$$\hat{I}_{f,N} = \int \hat{\pi}_N(\boldsymbol{x})f(\boldsymbol{x})d\boldsymbol{x} = \frac{1}{N}\sum_{i=1}^{N}f(\boldsymbol{x}^{(i)}). \tag{26}$$

According to the strong law of large numbers (SLLN) with $N \to +\infty$, $\hat{I}_{f,N}$ converges to I_f. The advantage of the MC sampling method is now clear. One can easily and efficiently estimate I_f and other statistical inferences based on the set of samples $\{\boldsymbol{x}^{(i)}; i = 1, 2, \ldots, N\}$. This means that parameter estimates can be determined by numerical evaluation of the expectation of the posterior distribution, a process which is easily implemented. MAP estimates are generated by finding the maximum of the histogram, which is implemented by finding the largest

element of an array, a process which is much easier than a multi–dimensional search, required by conventional Bayesian methods. In the proposed method discussed in this paper, we use the MAP approach. With Monte Carlo sampling techniques, it is also straightforward to generate estimates of variances, or estimates of the confidence regions corresponding to parameter estimates.

Unfortunately, it may be difficult or impossible to draw samples directly from the desired distribution $\pi(\boldsymbol{x})$. Instead, N samples are drawn from another "easy-to-sample" function $q(\boldsymbol{x})$, called the "importance function[1]," whose support includes that of $\pi(\boldsymbol{x})$. The histogram of these samples (particles) approximates the distribution $q(\boldsymbol{x})$. To generate a numerical approximation to the desired distribution $\pi(\boldsymbol{x})$, we use the *Bayesian importance sampling* method. The "importance weight" $w(\boldsymbol{x}^{(i)})$ is defined as follows:

$$w(\boldsymbol{x}^{(i)}) \propto \frac{\pi(\boldsymbol{x}^{(i)})}{q(\boldsymbol{x}^{(i)})} \tag{27}$$

such that the posterior distribution $\pi(\boldsymbol{x})$ can be approximated by a histogram defined as

$$\begin{aligned} \hat{\pi}_N(d\boldsymbol{x}) &= \frac{\sum_{i=1}^{N} w(\boldsymbol{x}^{(i)}) \delta_{\boldsymbol{x}^{(i)}}(d\boldsymbol{x})}{\sum_{j=1}^{N} w(\boldsymbol{x}^{(j)})}, \\ &= \sum_{i=1}^{N} \tilde{w}(\boldsymbol{x}^{(i)}) \delta_{\boldsymbol{x}^{(i)}}(d\boldsymbol{x}), \end{aligned} \tag{28}$$

where $\tilde{w}(\boldsymbol{x}^{(i)})$ is the normalized importance weight, given by

$$\tilde{w}(\boldsymbol{x}^{(i)}) = \frac{w(\boldsymbol{x}^{(i)})}{\sum_{j=1}^{N} w(\boldsymbol{x}^{(j)})}. \tag{29}$$

The expected value of the function $f(\boldsymbol{x})$ can now be estimated as follows:

$$\hat{I}_{f,N} = \int \hat{\pi}_N(\boldsymbol{x}) f(\boldsymbol{x}) d\boldsymbol{x} = \frac{1}{N} \sum_{i=1}^{N} w(\boldsymbol{x}^{(i)}) f(\boldsymbol{x}^{(i)}). \tag{30}$$

It can be shown [27] that even though $\hat{\pi}_N(\boldsymbol{x})$ is biased, the expectation $\hat{I}_{f,N}$ of any function $f(\boldsymbol{x})$ over $\hat{\pi}_N(\boldsymbol{x})$ converges to I_f as $N \to +\infty$. Once the histogram is available, parameter estimation can then proceed in the manner discussed above.

B. Sequential Update of The Posterior Distribution– Sequential Importance Sampling (SIS)

The idea of SIS, otherwise known as *particle filtering* (PF), is to update the weights $w(\boldsymbol{x}^{(i)})$ of the approximate posterior distribution in (28) recursively and sequentially, based on the arrival of new observations. It can be shown that an *optimal* importance function that minimizes the variance of the weights and has support including that of the target distribution is given by:

$$q_{optimal}(\cdot) = q(\boldsymbol{\alpha}_t^{(i)} | \boldsymbol{\alpha}_{t-1}^{(i)}, \boldsymbol{y}_t). \tag{31}$$

[1]Because $f(\boldsymbol{x})$ is sampled nonuniformly with the density $q(\boldsymbol{x})$, some samples $\boldsymbol{x}$ have more "importance" than others; hence, $q(\boldsymbol{x})$ is called the importance function.

Further, it is necessary for the recursive update of the weights that the importance function be factorizable as

$$q(\boldsymbol{\alpha}_{1:t}|\boldsymbol{y}_{1:t}) = q(\boldsymbol{\alpha}_{1:t-1}|\boldsymbol{y}_{1:t-1})q(\boldsymbol{\alpha}_t|\boldsymbol{\alpha}_{1:t-1}, \boldsymbol{y}_{1:t}). \tag{32}$$

The above has the form of (31). Denoting the importance weight $w^{(i)}(t)$ by

$$w^{(i)}(t) = \frac{\pi(\boldsymbol{\alpha}_{1:t})}{q(\boldsymbol{\alpha}_{1:t}|\boldsymbol{y}_{1:t})},$$

using the Markov properties of the model, the form of (31), and the *iid* assumptions on the noise variables, we have [22]

$$w^{(i)}(t) \quad = \quad \tilde{w}^{(i)}(t-1) \times \frac{p(\boldsymbol{y}_t|\boldsymbol{\alpha}_t^{(i)})p(\boldsymbol{\alpha}_t^{(i)}|\boldsymbol{\alpha}_{t-1}^{(i)})}{q(\boldsymbol{\alpha}_t^{(i)}|\boldsymbol{\alpha}_{1:t-1}^{(i)}, \boldsymbol{y}_{1:t})}, \tag{33}$$

where $\tilde{w}^{(i)}(t-1)$, which absorbs the normalizing component $p(\boldsymbol{y}_t|\boldsymbol{y}_{1:t-1})$, is defined as follows:

$$\tilde{w}^{(i)}(t-1) = \frac{w^{(i)}(t-1)}{\sum_{i=1}^{N} w^{(i)}(t-1)}. \tag{34}$$

Thus, because a recursive update on the weights is available, an approximation to the complete joint posterior distribution (28) is available at each time instant. This ultimately leads to improved performance over many other approaches for estimation, which rely solely on only a reduced set of (e.g., second-order) statistics.

A major difficulty with the SIS procedure is that the recursion of (33) degenerates quickly after a few iterations in such a way that all but a few of the normalized weights become very close to zero. As a result, any estimate based on these very few significant particles would show a large variance. Therefore, in addition to the use of the optimal importance function it is necessary to introduce other procedures to improve the recursion of (33).

Resampling is an idea to eliminate the trajectories of the weights which have weak normalized importance weights and to multiply trajectories with strong importance weights. The most popular resampling scheme is Sampling Importance Resampling (SIR), which resamples the particles according to their respective importance weights. It can be shown [28] that the resampling can be done very efficiently with order (N) operations. Unfortunately, the trajectories with high importance weights are statisically selected many times, limiting the true statistical diversity amongst the particles. This is the classical problem of depletion of samples, with the result that the cloud of particles may eventually collapse to a single particle.

An efficient way of limiting sample depletion consists of using a reversible jump MCMC step [19] [20] [23] on each particle at time t. The MCMC procedure provides new samples from the posterior distribution $\pi(\boldsymbol{\phi}(t)|\boldsymbol{y}(t))$, thus introducing statistical diversity amongst the particles. A pertinent aspect of the reversible jump process is that it is capable of exploring parameter spaces of varying dimension. This allows us to perform model order detection as well as estimation of the other parameters.

In summary, the proposed SIS approach is basically a combination of a sequential Bayesian importance sampling, sampling importance resampling, and an MCMC step. Note that the only

parameter in $\boldsymbol{\alpha}$ which is subjected to the sampling procedure is the DOA vector $\boldsymbol{\phi}$. The model order $k(t)$ is sampled using the reversible jump process to be described, the desired amplitudes (which give the source waveforms), are estimated from (17), and the variances are estimated according to (21) and (22). We summarize these steps in the following table:

Sequential Importance Sampling Algorithm

Initialization

For time $t = 1$,

- sample N particles $\boldsymbol{\phi}^{(i)}, i = 1, \ldots, N$ from $q(\cdot|\cdot)$.
- initialize the weights $w^{(i)}$, $i = 1, ..., N$ to $\frac{\pi(\boldsymbol{\phi}^{(i)})}{q(\boldsymbol{\phi}^{(i)})}$.
- normalize the weights to $\tilde{w}^{(i)}(t) = \frac{w^{(i)}(t)}{\sum_{j=1}^{N} w^{(j)}(t)}$.

Then for $t = 2, 3, ...$

1. *Sequential Importance Sampling Step*

(a) Sample N particles of $\boldsymbol{\phi}_t^{(i)}$ for $i = 1, 2, \ldots, N$ from the optimal importance function given from (31) as follows:

$$\boldsymbol{\phi}_t^{(i)} \sim q(\boldsymbol{\phi}_t^{(i)}|\boldsymbol{\phi}_{1:t-1}^{(i)}, \boldsymbol{y}_{1:t}). \tag{35}$$

(b) Evaluate the importance weights for N particles as follows:

$$w^{(i)}(t) = \tilde{w}^{(i)}(t-1) \times \frac{p(\boldsymbol{y}_t|\boldsymbol{\phi}_t^{(i)})p(\boldsymbol{\phi}_t^{(i)}|\boldsymbol{\phi}_{t-1}^{(i)})}{q(\boldsymbol{\phi}_t^{(i)}|\boldsymbol{\phi}_{1:t-1}^{(i)}, \boldsymbol{y}_{1:t})},$$

and hence the normalized importance weights are given as follows:

$$\tilde{w}^{(i)}(t) = \frac{w^{(i)}(t)}{\sum_{j=1}^{N} w^{(j)}(t)}.$$

2. *Sampling Importance Resampling Step*

Multiply/Suppress the particles $\boldsymbol{\phi}^{(i)}(t)$ respectively with high/low importance weights $\tilde{w}^{(i)}(t)$ to obtain N random samples approximately distributed according to $\pi(\boldsymbol{\phi}_{1:t}^{(i)})$.

- Sample a vector $\boldsymbol{l}$ distributed as:

$$P(l(j) = i) = w^{(i)}(t).$$

- Resample the particles with the index vector:

$$\boldsymbol{\phi}_{1:k}^{(i)} = \boldsymbol{\phi}_{1:k}^{(l(i))}.$$

- Re-assign all the weights to $w^{(i)}(t) = \frac{1}{N}$.

3. *MCMC Step*

Follow the MCMC procedure to be described in Section IV to introduce diversity of the particles and to facilitate detection of model order. ■

Note that the MCMC process normally requires a "burn–in" period for the chain to reach equilibrium. However in this case, this is not required, since the particles are already distributed according to the desired posterior distribution, which is the invariant distribution of the chain, before application of the MCMC procedure.

IV. The Reversible Jump MCMC Diversity Step

The reversible jump MCMC (RJMCMC) process [23], which is a variation of the Metropolis-Hasting (M-H) algorithm [29], can be used for model order detection. While one could sample the subspace corresponding to a range of model orders independently, the computational cost of such a scheme can be very large, since the same effort is allocated to all model orders, even though some models will have a very low posterior probability. In contrast, the RJMCMC algorithm directly samples the model order $k(t)$ from the joint posterior distribution, by jumping between subspaces of different dimensions, thus visiting all relevant model orders. The procedure is more computationally efficient, since the most likely model orders are visited most often, and hence correspondingly less effort is spent on model orders with lower probability. The RJMCMC algorithm inherently sets up a Markov chain which is capable of jumping between model orders, yet whose invariant distribution corresponds to the joint posterior $\pi(\boldsymbol{\phi}, k)$ of interest.

The algorithm itself is similar to the conventional Metropolis–Hastings algorithm [29]. At each iteration, the algorithm proposes a candidate from a set of candidate distribution functions. These functions are designed to change the model order. At each iteration, a candidate distribution $q(\cdot)$ is randomly chosen, and a sample candidate $\boldsymbol{\phi}^\star$ of size $k^\star$ is obtained by sampling $q(\cdot)$. This candidate sample will be accepted with probability α defined as

$$\alpha((\boldsymbol{\phi}^\star, k^\star), (\boldsymbol{\phi}, k)) = \min\{r((\boldsymbol{\phi}^\star, k^\star), (\boldsymbol{\phi}, k)), 1\}, \tag{36}$$

with the acceptance ratio r being defined as

$$r((\boldsymbol{\phi}^\star, k^\star), (\boldsymbol{\phi}, k)) = \frac{\boldsymbol{\pi}(\boldsymbol{\phi}^\star, k^\star) q(\boldsymbol{\phi}, k)}{\boldsymbol{\pi}(\boldsymbol{\phi}, k) q(\boldsymbol{\phi}^\star, k^\star)} \boldsymbol{J}((\boldsymbol{\phi}^\star, k^\star), (\boldsymbol{\phi}, k)). \tag{37}$$

If the candidate is accepted, the chain takes on the new state; otherwise the chain remains at the current state.

The term $\boldsymbol{J}((\boldsymbol{\phi}^\star, k^\star), (\boldsymbol{\phi}, k))$ is the Jacobian of the transformation, required to reconcile the total probability between spaces of different dimensions so that the reversibility condition [2] is satisfied, and is defined [30] as

$$\boldsymbol{J}((\boldsymbol{\phi}^\star, k^\star), (\boldsymbol{\phi}, k)) = \left| \frac{\partial \boldsymbol{\phi}^\star}{\partial \boldsymbol{\phi}} \right|. \tag{38}$$

It may be be verified that for this study, $\boldsymbol{J}(\cdot|\cdot) = 1$. The most widely used candidate functions are the birth/death complementary moves. When the death move is selected, the algorithm

[2]The reversibility condition states that the probability distribution of the Markov chain entering a particular state is equal to the probability of the chain leaving the state. The reversibility condition is sufficient for the states of the chain to assume its invariant distribution. The procedure involving (36) and (37) ensures the invariant distribution of the chain is indeed the desired joint posterior, in model order and parameters.

proposes a candidate in the model of lower dimension, as opposed to the birth move, which proposes a candidate of higher dimension. However, if neither move is selected, the update move, which leaves the model order unchanged, is executed. The probabilities for choosing each move are denoted u_k, b_k and d_k, respectively, such that $u_k + b_k + d_k = 1$ for all k. In this case, we choose the probability of a jump to be between 0.5 and 1 at each iteration [23].

It is clear that once the joint posterior distribution $\hat{\pi}_N(\boldsymbol{\alpha}(t), k(t))$ is available from the RJMCMC procedure, the model order k can be determined by marginalizing with respect to $\boldsymbol{\alpha}(t)$, leaving only $\hat{\pi}_N(k(t))$. Then the estimate of model order $\hat{k}(t)$ can be determined using, e.g., a MAP procedure.

These methods were first applied to engineering problems by Andrieu and Godsill [25] [31] [32] [33] for the detection and estimation of parameters in white noise. The overall description of the RJMCMC algorithm is determined by the choice of moves at each iteration. This description is summarized as follows.

Reversible Jump MCMC

1. Current state of the chain = current state of the particles $(k(t), \boldsymbol{\phi^{(i)}}(t))$.
2. Iteration t for the ith particle, $i = 1, ..., N$
   - Sample $u \sim U$, where U is a uniform distribution over $[0, 1]$,
   - if $(u < b_k)$ then execute a "birth move",
   - else if $(u < b_k + d_k)$ then execute a "death move",
   - else, execute an update move .
3. $t \leftarrow t + 1$, goto step 2

■

A. Update Move

In this move, the model order is kept fixed, i.e., $k(t) = k(t-1)$. The steps are summarized as follows:

1. To introduce diversity of the particles, we execute one iteration of the Metropolis Hastings MCMC algorithm [29]. This procedure generates a new set of N particles distributed according to the desired posterior distribution $\pi(\boldsymbol{\alpha})$ given by (19):

for $i = 1, \ldots, N$

(a) Sample a candidate DOA $\phi^\star$ from the following proposal distribution:

$$q(\boldsymbol{\phi}^{(i)}(t)|\boldsymbol{\phi}^{(i)}(t-1)) = \mathcal{N}(\boldsymbol{\phi}^{(i)}(t-1), \sigma_v^2 \boldsymbol{I}_{k(t)}), \tag{39}$$

which has the form of (35).

(b) evaluate the acceptance ratio by substituting (39) and (19) into (37) as follows:

$$r_{update} = \frac{\exp\left[-\frac{1}{\sigma_w^2}\boldsymbol{y}^H(t)\boldsymbol{P}_S^{\perp}(\phi^\star)\boldsymbol{y}(t)\right]}{\exp\left[-\frac{1}{\sigma_w^2}\boldsymbol{y}^H(t)\boldsymbol{P}_S^{\perp}(\phi^{(i)}(t))\boldsymbol{y}(t)\right]}, \tag{40}$$

(c) accept the candidate $\boldsymbol{\phi}^{\star}$ with the probability:

$$\eta_{update} = \min\{r_{update}, 1\}. \tag{41}$$

2. Estimate $\hat{\boldsymbol{\phi}}(t)$ using a MAP procedure from the histogram obtained from the particles.
3. Using $\hat{\boldsymbol{\phi}}(t)$, estimate the amplitudes $\boldsymbol{a}(t)$ according to (17).
4. Estimate the noise variances σ_v^2 and σ_w^2 according to (21) and (22), respectively, for use in (39) and (40).

B. Birth/Death moves

The procedure for executing the birth/death moves is similar to that of the update move discussed above. However, the birth move proposes a candidate in a higher dimension model, whereas the death move proposes a candidate in a lower dimension model. In the birth move, we assume that the current state is $(\boldsymbol{\phi}_k, k)$ and we wish to determine whether the next state is $\left(\boldsymbol{\phi}_{k+1}, k+1\right)$ at the next iteration. This involves the addition of a new source ϕ_c, which is proposed at random from the prior distribution for the directions of arrival such that:

$$\boldsymbol{\phi}^{\star}_{k(t)+1} = \left[\boldsymbol{\phi}_k(t) | \phi_c\right]. \tag{42}$$

Then, the acceptance ratio corresponding to (40) for the birth move is:

$$r_{birth} = \frac{\exp\left[-\frac{1}{\sigma_w^2}\boldsymbol{y}^H(t)\boldsymbol{P}_S^{\perp}(\phi^{\star}_{k+1})\boldsymbol{y}(t)\right]}{\exp\left[-\frac{1}{\sigma_w^2}\boldsymbol{y}^H(t)\boldsymbol{P}_S^{\perp}(\phi_k^{(i)})\boldsymbol{y}(t)\right]} \times \frac{1}{(1+\delta^2)(k+1)}, \tag{43}$$

where the $\boldsymbol{\phi}^{\star}_{k+1}$ will be accepted with a probability:

$$\eta_{birth} = \min\{r_{birth}, 1\}. \tag{44}$$

The underlying Markov chain must be reversible with respect to moves across subspaces of different model order, so that the desired invariant distribution of the chain with respect to model order is preserved by the MCMC algorithm. That is, the probability of moving from model order k to $k+1$ must be equal to that of moving from $k+1$ to k. Thus, there must also be the death move in which a source in the current state $\left(\boldsymbol{\phi}_{k+1}, k+1\right)$ is randomly selected to be removed such that the next state becomes $(\boldsymbol{\phi}_k, k)$ at the next iteration. In order to preserve reversibility, the acceptance ratio for the death move must be [23]

$$r_{death} = \frac{1}{r_{birth}}, \tag{45}$$

and a new candidate of dimension k is accepted with probability:

$$\eta_{death} = \min\{\frac{1}{r_{death}}, 1\}. \tag{46}$$

The schemas for the birth and death moves are similar to those for the update move.

Parameter	M	k	σ_v^2	$\boldsymbol{a}(0)$
Value	8	2	$(10)^{\circ^2}$	$[10, 8]$

TABLE 5.1

Parameters of the state-space model for simulating the data for Experiment 1.

V. Simulation Results

The proposed PF algorithm is now applied to three sets of simulation data, generated for $k = 2$ sources with the parameter values listed in Tables 5.1 and 5.6, respectively. A uniform linear array composed of $M = 8$ elements with a half–wavelength spacing of the elements is used in all the simulations. In each experiment, $N = 300$ particles are used.

In the first experiment, the ability of the proposed method to simultaneously track and detect the number of sources as well as extract the source waveforms is demonstrated. The variance of the observation noise $\sigma_w^2(t)$ is made nonstationary, with corresponding SNR values shown in Table 5.3. In this experiment, one of the sources vanishes suddenly. The proposed particle filtering (PF) method is compared with the extended Kalman Filter (EKF) [14][24], which linearizes the highly nonlinear observation model in (6).

In the second experiment, the PF method is compared with the LPA-beamformer [1] [2]. The LPA- beamformer has the ability to adapt to a target direction which changes throughout the observation interval.

In the last experiment, a smoother track is used to compare the proposed method with the LPA-beamformer. This is a more favorable case for the latter method. In this case, the DOAs tracks correspond to two sinusoidal functions.

A. Experiment 1 : Joint DOA tracking and detection of unknown sources

In the first experiment, the DOA tracks of the two sources correspond to autogressive (AR) processes whose coefficients represent a 10th–order low–pass Butterworth filter, with normalized cutoff frequency 0.1, variance σ_v^2, and with AR coefficients which are specified in Table 5.2. These simulated tracks are representative of a difficult but realistic tracking scenario in real life. Likewise, the source waveforms are AR processes, generated from a 10th–order low–pass butterworth filter with normalized cutoff frequency 0.3, whose coefficients are also listed in Table 5.2. Figure 1 depicts the locations of the roots of the AR coefficients used for the generation of DOAs and signal amplitudes, respectively. The initial value $\boldsymbol{\phi}(0)$ is $[-20^\circ, 30^\circ]$ and the initial SNR is about 18.56 dB for both sources. 300 snapshots are generated. One of the sources vanishes at $t = 200$. In order to show the robustness of the PF method in a nonstationary noise environment, the observation noise is generated such that the variances are varying or nonstationary in different regions of time. The average SNRs in the different time regions are summarized in Table 5.3.

In this experiment, the EKF simulation assumes the number of sources $k = 2$ is known and

AR coefficients for DOA generation	AR coefficients for signal amplitude generation
1	1
-7.9923	-3.9877
28.9122	8.0944
-62.3154	-10.4736
88.5877	9.4233
-86.7671	-6.0842
59.2810	2.8353
-27.8903	-0.9364
8.6457	0.2089
-1.5942	-0.0283
0.1328	0.0018

TABLE 5.2

THE AR COEFFICIENTS FOR THE GENERATION OF THE DOA AND SIGNAL AMPLITUDE PROCESSES.

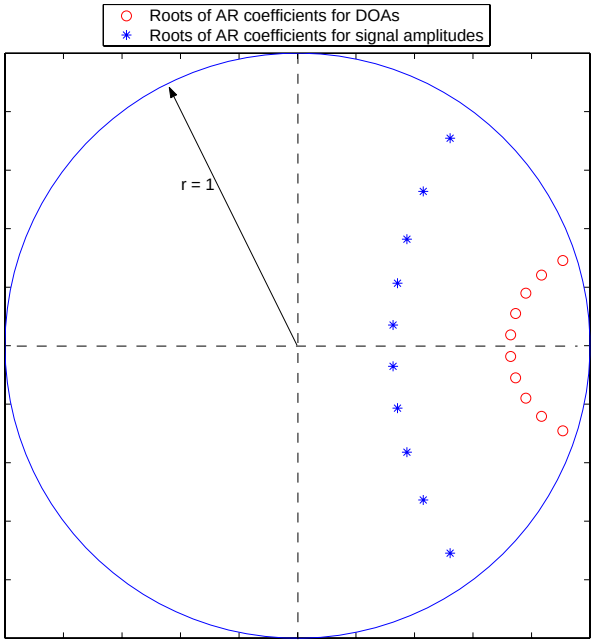

Fig. 1. The roots of the AR processes.

Time range	SNR (dB)
1-100	18.56
101-200	15.32
201-300	19.78

TABLE 5.3

THE AVERAGE SNRS IN THE DIFFERENT TIME RANGES.

constant, but the PF method is capable of detecting the number of sources sequentially, and therefore does not require knowledge of k. Unlike the PF method, the EKF requires the exact AR process model, and the noise covariance matrices.

The proposed algorithm randomly initializes the unknown parameters and assigns the model order $k(0)$ to $k_{\max} = M - 1 = 7$, where $k_{\max}$ is the maximum allowable model order.

First, we consider the performance of the PF approach in detecting model order. The instantaneous model order estimate versus time is shown in Figure 2. We see that the detection process takes about 10 snapshots to converge to the true model order $k = 2$, and that the vanishing source is properly detected at $t = 200$.

Even though the objective of this work is to recover the amplitudes, the DOA estimation process is a critical step in determining the source waveforms. This is because the MAP amplitude estimate of (17) requires the $\boldsymbol{\phi}$'s. Thus, we first consider a comparison of the DOA estimation performance of the PF method versus that of the EKF. As shown in Figure 3, it is seen the PF method significantly outperforms the EKF in terms of accuracy in tracking the DOAs. In the region $0 < t < 20$, the PF approach is recovering from a transient due to the tracks being initialized to the incorrect values. The relatively poor performance of the EKF is due in part to the highly nonstationary behavior of the tracks. The performance of the PF method degrades over the interval $160 \leq t \leq 180$ where the sources are very closely spaced, as shown in Figure 4 (This figure is a zoomed version of Figure 3, for the region $t = [151, 209]$). This behavior is expected since the matrix $\boldsymbol{S}(\boldsymbol{\phi})$ becomes poorly conditioned in this case. It is seen that after $t = 200$ when source 1 vanishes, the PF method detects the change in model order, and subsequently, produces accurate DOA estimates, as shown in Figures 3 and 4. However, since the EKF has no facility for model order detection, it assumes there are still $k = 2$ sources during this interval. As a result, because of this error in the model, the DOA estimates produced by the EKF are grossly in error.

We now consider the performance of the source waveform recovery. The performances of both approaches are directly dependent on the accuracy of the DOA estimation. Figure 5 shows amplitude waveforms recovered using three different methods. The first uses the PF approach to determine the DOAs at each time instant, and then uses (17) to generate the corresponding amplitudes. The second is similar, except it uses the EKF to generate the DOAs. In this case, the amplitudes are determined using (17) with $\delta^2 = 0$. The third method uses the EKF to estimate the DOAs, but then uses a conventional beamformer method [15] to compute of a set of adaptive weights based on the estimated DOAs from the EKF procedure. The source waveforms $\hat{\boldsymbol{a}}(t)$ are then recovered from the output of the beamformer. By assuming that the two sources are the targets to be protected, we can compute the weights, $\boldsymbol{u}(t)$, using a constrained optimization procedure as follows

$$\begin{aligned} u_{opt}(t) = &\arg\min_{\boldsymbol{u}(t)} \boldsymbol{u}^H(t)\hat{\boldsymbol{R}}(t)\boldsymbol{u}(t) \\ &\mathbf{s.t.}\, \boldsymbol{C}(t)\boldsymbol{u}(t) = \boldsymbol{c}, \end{aligned} \tag{47}$$

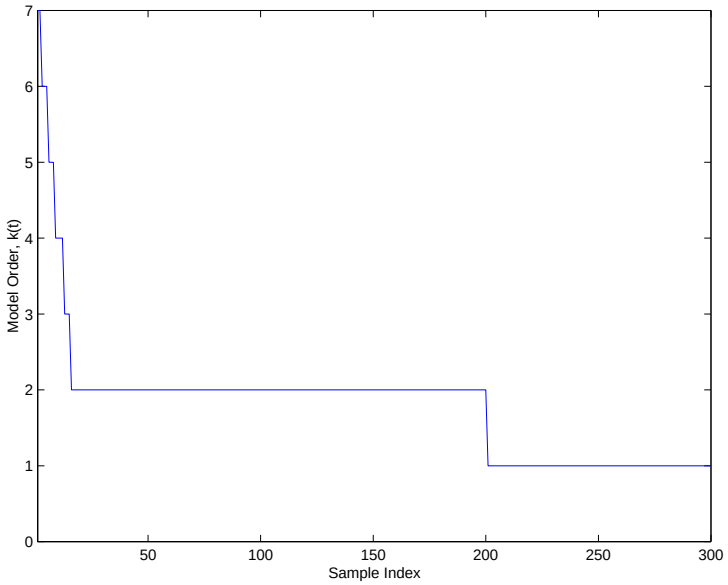

Fig. 2. Sequential estimates of model order for Experiment 1.

where $\hat{\boldsymbol{R}}(t)$ is a sample covariance matrix, recursively updated as

$$\hat{\boldsymbol{R}}(t) = \hat{\boldsymbol{R}}(t-1) + \boldsymbol{y}(t)\boldsymbol{y}^H(t), \tag{48}$$

$\boldsymbol{C}(t)$ is the constraint matrix, the columns of which are the steering vectors evaluated at the estimates $\hat{\boldsymbol{\phi}}(t)$, and $\boldsymbol{c}$ is a column of constraining values. In this particular simulation, all constraining values are set to one, that is, all targets are kept intact at unity gain. The beamformer output $\hat{\boldsymbol{a}}(t)$ is given as $\hat{\boldsymbol{a}}(t) = \boldsymbol{u}_{opt}^H(t)\boldsymbol{y}(t)$. The respective DOA estimates used by the PF and EKF approaches are those shown in Figure 3.

Given the relatively poor performance of the EKF with regard to DOA estimation, the signal extraction for both the EKF approaches is adversely affected, as shown in Figure 5. It is seen that the waveforms recovered using the DOA estimates from the particle filter are significantly improved over those given using the EKF. It is only in the region $160 < t < 180$, where the DOAs are extremely close together, that the particle filter approach deteriorates. The improved behaviour of the PF method is in spite of the additional information (i.e., the covariance matrices and the model order) that are required by the EKF method. Even though the EKF is simple and relatively easy to implement, the linearization used in the EKF in the measurement and/or state prediction can introduce a bias, and the covariance computation based on a series expansion is not always accurate [14]. In addition, unless accurate estimates of all other important parameters are given, the EKF will not perform as intended. Furthermore, a significant advantage of the proposed method is that it is capable of detecting the instantaneous number of sources, which is crucial in signal extraction, especially when the number of sources is time-varying.

B. Experiment 2: Comparison with the LPA beamformer

In the second experiment, the PF method is compared with the LPA-beamformer [1] [2]. The DOA tracks and the two source waveforms are generated as in experiment 1, with initial values

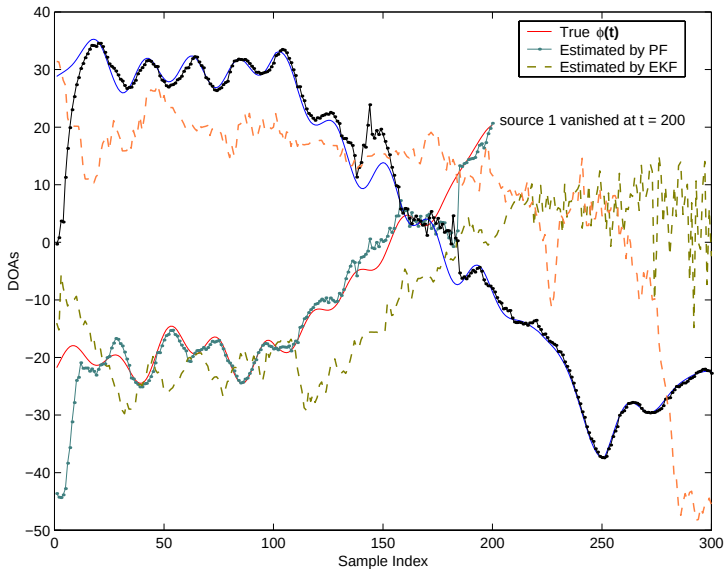

Fig. 3. Comparison of DOA tracking performance for the PF and the EKF methods, for Experiment 1.

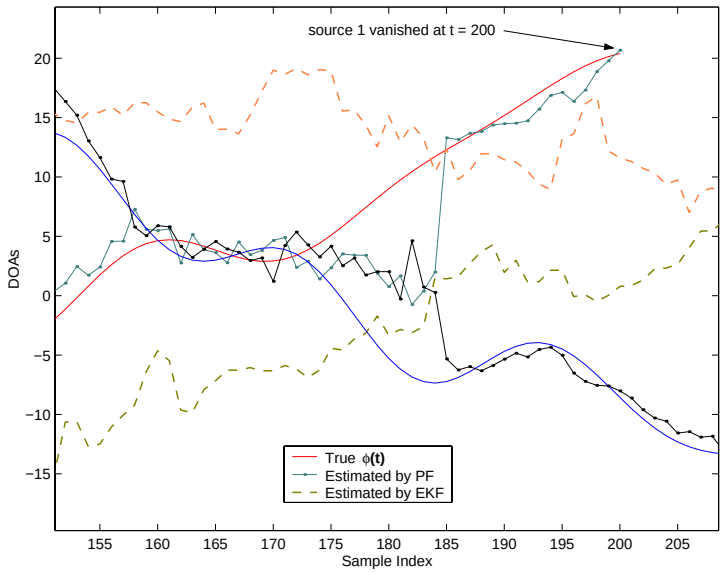

Fig. 4. A zoomed version of Figure 3, from sample $t = 151$ to $t = 209$, highlighting the region where the source disappears.

$\boldsymbol{\phi}(0) = [0°, -20°]$, and $k(0) = k_{\max}$, and with the other parameters listed as before in Table 5.1. Here, the DOA tracks cross each other at about $t = 140$, and the model order remains fixed at $k = 2$ throughout the entire observation interval. In this experiment, the observation noise variance is constant throughout the observation interval. The signal amplitudes are extracted using (17) directly for the PF method. For the LPA method, the sources are extracted using the beamformer approach described by (47) and (48).

Figure 6 shows the convergence of the model order estimate from its initial value of $k_{\max}$ to the true value $k = 2$. As seen, it takes about 10 snapshots for the PF model order detection scheme to converge to the correct value. The performance for both the DOA and waveform estimation processes for the PF and the LPA methods are shown in Figures 7 and 8, respectively. It is

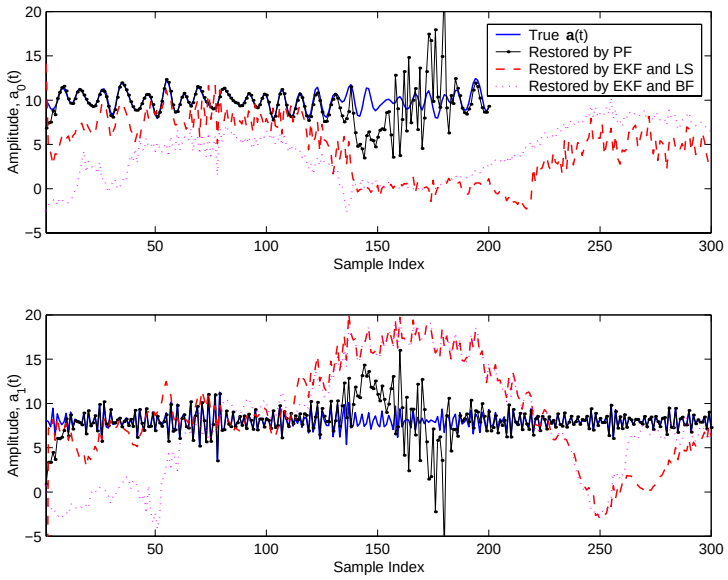

Fig. 5. Comparison of the waveform extraction performance of the PF method and the LS and beamforming approaches based on the EKF, for Experiment 1. Top: recovered source waveform for source 0, Bottom: same for source 1.

seen that the observations concerning the relative performance of the PF vs. EKF approaches in Experiment 1 persist in this experiment also.

The LPA-beamformer technique was developed to relax the assumption that DOAs are constant within the entire observation period, as is required with conventional beamformers. It accommodates DOA variation within a sliding time window by modelling the DOA trajectory vs. time as a polynomial, whose coefficients must be estimated. Like the EKF, the LPA-beamformer assumes the number of sources is known and constant throughout the entire observation period. The length of the sliding window for the LPA-beamformer for this experiment is $L = 15$, and a first-order polynomial is used to track the changing DOAs within the window[3].

As shown in Figure 7, the estimated tracks produced by the LPA-beamformer are not close to the true tracks until they are well-separated and relatively smooth, as is the case for $t \geq 150$. The degraded performance of the LPA-beamformer relative to the PF approach can be explained by the fact that the DOA motion within the sliding window violates the assumption of smooth and linear behaviour. Since the performance of the LPA-beamformer is somewhat degraded with regard to DOA estimation, the signal extraction is also adversely affected, as shown in Figure 8.

Tables 5.4 and 5.5 provide a quantitative measure of the performance of the various algorithms in terms of the MSE of the estimated DOAs and source waveforms. As expected, the MSE for the DOA and amplitude estimates in the periods $t \in [1, 114]$ and $t \in [251, 300]$ are small, respectively, for the PF method. In contrast, the errors are comparatively larger for the LPA approaches. During $t \in [115, 250]$ when the tracks are very close, the DOA estimation MSE

[3]The first-order polynomial was chosen because it gave the best performance. Higher-order polynomials have the potential to track changing directions better, but degrade in performance because more coefficients must be estimated.

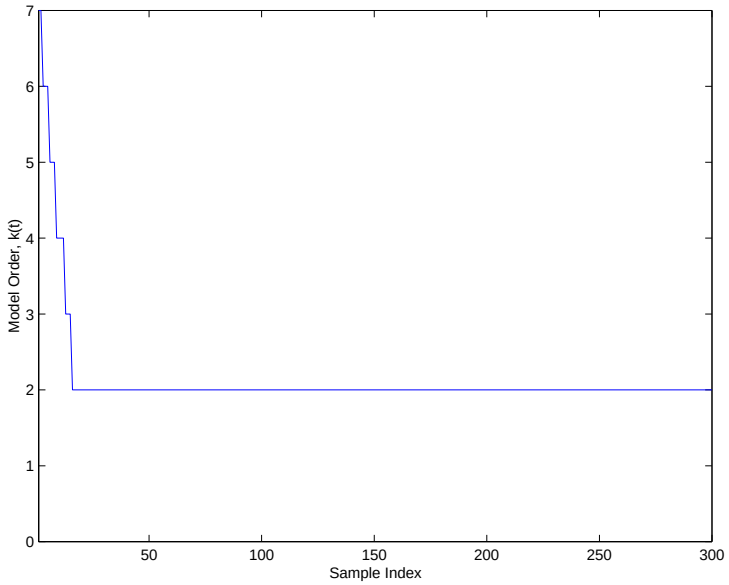

Fig. 6. Sequential estimates of model order for Experiment 2, using the PF method.

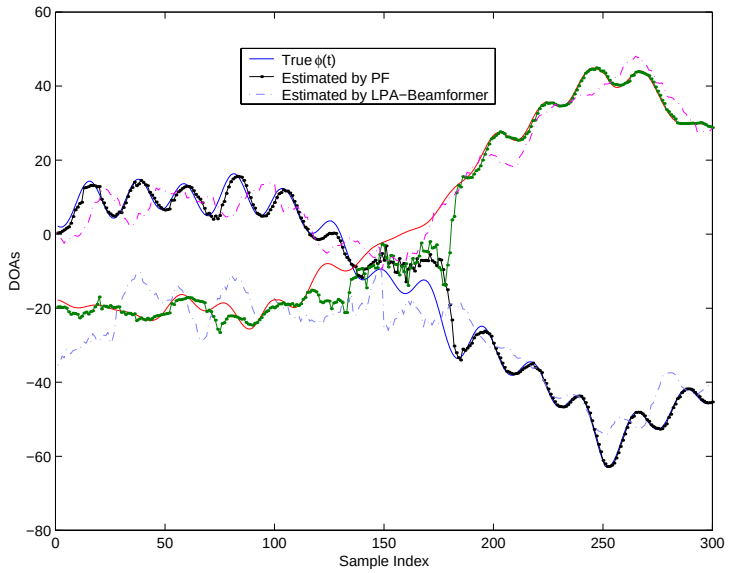

Fig. 7. Comparison of the DOA tracking performance for the PF method and the LPA approach for Experiment 2.

on average is far better than that for amplitude estimation for the PF method, implying that amplitude estimation is very sensitive to DOA estimation, when the DOA tracks are close. Nevertheless, these errors are still far smaller for the PF method than those produced by the other approaches.

We will include MSEs for different numbers of particles, e.g., in Tables 5.4 and 5.5.

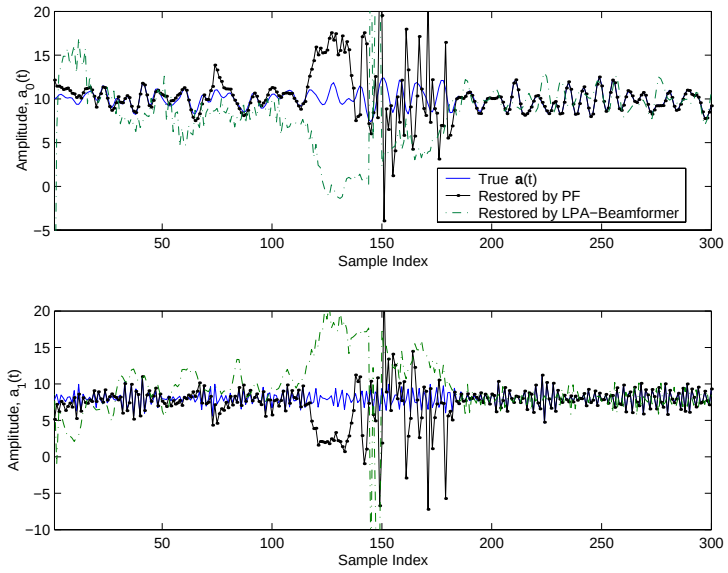

Fig. 8. Comparison of the waveform extraction performance for the PF method and the LPA approach for Experiment 2.

MSE (dB)	$t \in [1, 114]$	$t \in [115, 250]$	$t \in [251, 300]$
PF	-27.36, -30.28	-10.34, -18.22	-32.97, -40.45
LPA-beamformer	-20.01, -18.21	-8.23, -6.12	-24.89, -32.91

TABLE 5.4

THE MSE BETWEEN THE TRUE AND ESTIMATED DOAS OVER 50 INDEPENDENT TRIALS FOR THE PF METHOD AND THE LPA-BEAMFORMER, FOR EXPERIMENT 2.

C. Experiment 3: Comparison between the PF method and the LPA-beamformer

In this experiment, the two DOA tracks are smooth sinusoidal functions, given by

$$\boldsymbol{\phi}(t) = \boldsymbol{\phi}(0) + 10 \sin\left(\frac{10\pi t}{300}\right), \quad t = 1, ..., 300,$$

where $\boldsymbol{\phi}(0) = (20, -20)^\circ$, are used to compare the tracking performance and hence the signal extraction of the proposed method with that of the LPA-beamformer. The amplitudes are generated using AR processes as in the previous experiments. The number of sources is assumed known and constant. The other parameters used in this simulation can be found in Table 5.6.

Figures 9 and 10 show the comparison between the proposed method and the LPA-beamformer in terms of DOA tracking and signal extraction, respectively. According to these figures, these methods provide comparable performance in both respects, although the PF method is slightly better. Table 5.7 summarizes the MSE of the DOA estimation and signal extraction for these methods over 50 independent trials.

The LPA-beamformer, which relies on a first-order linear model to track slowly fluctuating DOAs, suffers from model mismatch in highly nonstationary conditions. If the assumptions for the LPA-beamformer are violated, i.e. the tracks are not smooth and moderately nonstationary,

MSE (dB)	$t \in [1, 114]$	$t \in [115, 250]$	$t \in [251, 300]$
PF	-17.28, -18.00	-5.63, -6.46	-24.28, -26.58
LPA-beamformer	10.76, -11.56	8.45, 13.67	-17.88, -19.01

TABLE 5.5

THE MSE BETWEEN THE TRUE AND ESTIMATED AMPLITUDES OVER 50 INDEPENDENT TRIALS FOR THE PF AND BEAMFORMING APPROACHES, FOR EXPERIMENT 2.

Parameter	M	K	$SNR(dB)$	$\boldsymbol{\phi}(0)$	$\boldsymbol{a}(0)$
Value	8	2	15	$[-20°, 20°]$	$[8, 10]$

TABLE 5.6

PARAMETERS OF THE STATE-SPACE MODEL FOR SIMULATING THE DATA FOR EXPERIMENT 3.

the LPA-beamformer performs poorly with regard to DOA tracking, and hence in extracting signals. However, we have seen that the PF method is capable of DOA tracking and source extraction in highly nonstationary situations. On the other hand, if all conditions favor the LPA-beamformer, as in this experiment, then it is seen that both methods have comparable performance, and the LPA-beamformer is then preferred over the PF method because it is less computationally intensive.

D. Discussion

In addition to the reasons previously cited, the superior performance of the PF method is in part, through (33), due to the availability of an approximate *instantaneous* joint posterior distribution of all the relevant parameters at each time instant. This is in contrast to previous

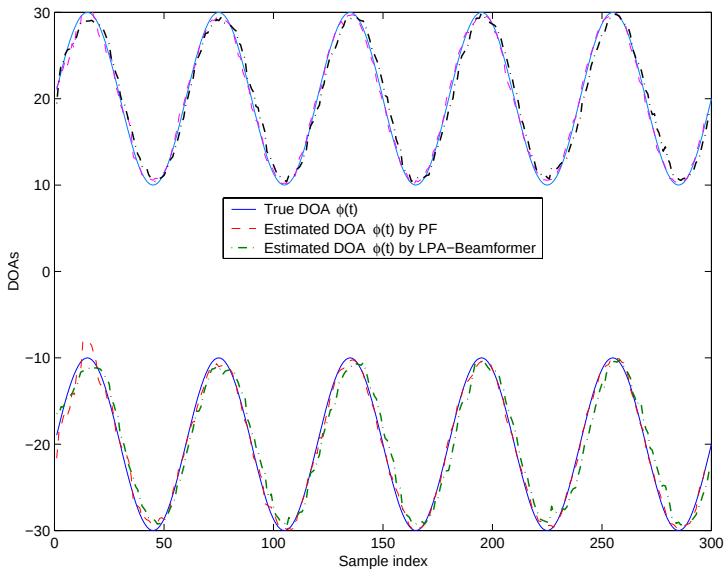

Fig. 9. Comparison of the DOA tracking performance for the PF method and the LPA-beamformer.

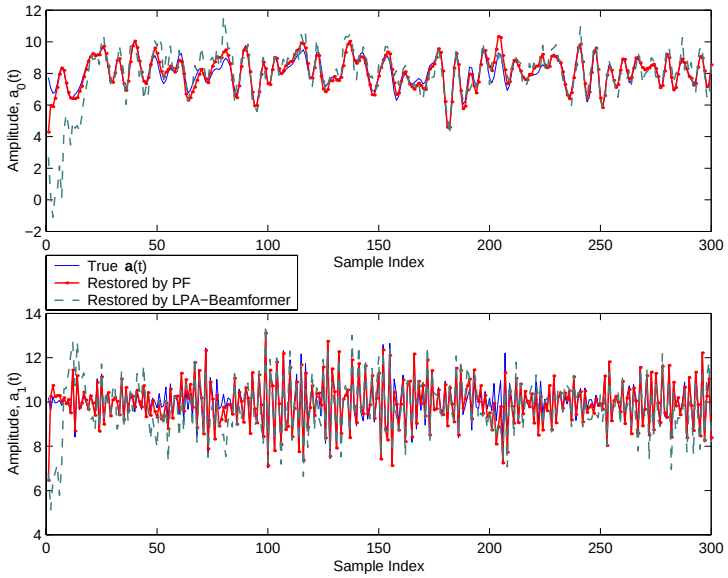

Fig. 10. Comparison of the waveform extraction process for the PF method and the LPA beamformer.

MSE (dB)	MSE for DOA Estimation (dB)	MSE for DOA Estimation (dB)
PF	-24.24, -26.00	-16.63, -18.37
LPA-beamformer	-21.30, -24.28	-14.02, -17.60

TABLE 5.7

THE MSE FOR DOA ESTIMATION AND SIGNAL EXTRACTION FOR THE PF AND THE LPA-BEAMFORMER APPROACHES, OVER 50 INDEPENDENT TRIALS FOR EXPERIMENT 3.

methods which are based on accumulating statistics by time averaging. This technique assumes stationarity of the underlying process over an adequate time interval. This leads to degradation in performance in situations where significant degrees of nonstationarity exist. On the other hand, the PF method does not need to accumulate statistics by time averaging, since it has the entire posterior distribution available at each instant of time.

A further advantage of the proposed PF method is that confidence regions of the parameter estimates can be easily evaluated. This is a consequence of the fact that an approximation to the posterior distribution is available at each time instant. An example of a posterior distribution of the DOA estimates, from which confidence regions can be obtained, corresponding arbitrarily to the 245th DOA sample in experiment 2 (see Figure 7), is shown in Figure 11.

Note that once the $\boldsymbol{\phi}$'s have been estimated, the waveforms could also be obtained using a Kalman filter. The proposed MAP procedure and the Kalman filter should give almost equivalent performance, since the MAP method is optimum in a Bayesian sense, while the Kalman filter is optimum in a least-squares sense.

It is easily shown that as $N \rightarrow \infty$, where N is the number of particles, the global optimum of the desired posterior distribution coincides with the most heavy-weighted histogram bin corresponding to the particles. In practice, the global optimum is achieved within a histogram

bin-width with finite N with high probability. Thus, the global optimum can be attained by a simple search, instead of a complicated global optimization over a multi-modal surface.

The computational expense of the particle filter approach is fairly high, requiring $\mathcal{O}(N)$ function evaluations each time step. However, the evaluation of the particles is easily parallelizable, and this order of computation does not necessarily compare unfavourably with that of a global procedure required to estimate the multiple DOAs for the beamformer. Furthermore, the relative computational expense of the method is offset by its advantages; namely, a joint detection capability and improved performance in nonstationary environments.

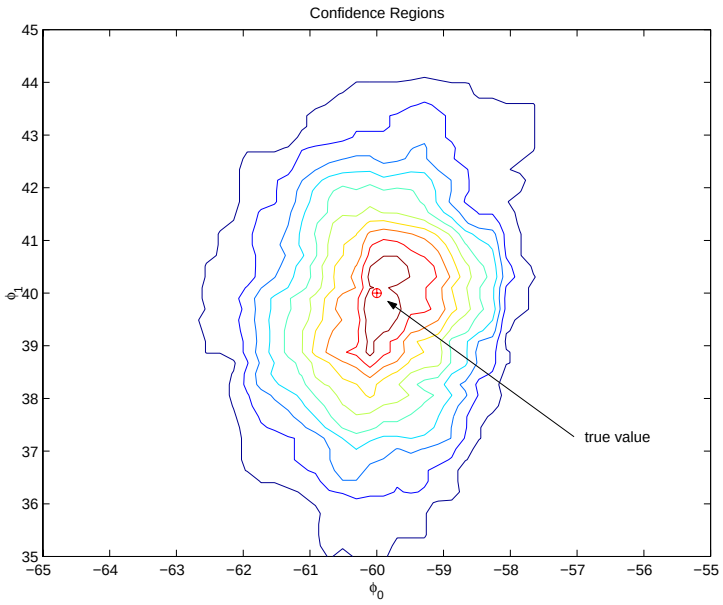

(a)

Fig. 11. Contours of the approximate posterior distribution of the DOAs with true values at $[-60^o, 40^o]$.

Finally, we investigate the effect of the number of particles N on the performance of the proposed PF method. Table 5.8 compares the MSE between the true and estimated DOAs for different values of N using the experimental configuration of Experiment 2. As can be seen, the algorithm does not improve significantly as N increases from 300 to 500, whereas the computational load is increased by approximately 60%. However, we notice that performance does deteriorate as N drops to 100 particles. In other words, one can tradeoff the performance of the algorithm and the complexity of the implementation by adjusting the number of particles N. The use of the optimal importance function (39) is effective in reducing the required number of particles.

VI. Conclusion

In this paper, an alternative to the classical beamforming approach, preceded by angle-only estimation, for recovering multiple desired signals and tracking their sources in nonstationary environments in the presence of interference using arrays of sensors is presented. The proposed method implements sequential Markov Chain Monte Carlo (MCMC) estimation, also known as

MSE (dB)	$t \in [1, 114]$	$t \in [115, 250]$	$t \in [251, 300]$
N = 500	-28.37, -31.76	-10.89, -19.10	-34.01, -43.39
N = 300	-27.36, -30.28	-10.34, -18.22	-32.97, -40.45
N = 100	-20.85, -25.01	-9.90, -14.56	-28.19, -34.94

TABLE 5.8

The MSE between the true and estimated DOAs by PF for 50 independent trials for different number of particles N for Experiment 2.

particle filtering. Unlike the traditional beamforming methods, the proposed method is able to track rapidly moving sources and recover their waveforms.

In addition, the proposed method simultaneously detects the number of unknown sources. In contrast to other methods like EKF and the LPA-beamformer, the proposed method is more robust to nonlinearity in the data model and less sensitive to model selection. The simulations have shown that the proposed method has superior performance in terms of DOA tracking ability and signal recovery, relative to other methods. A seamless Bayesian framework for detecting the number of sources as well as for tracking their DOAs was presented. Simulation results were also presented to show the benefits of the new algorithm in terms of estimation accuracy and diversity.

References

[1] A. Gershman, "Robust Adaptive Beamforming in Sensor Arrays," in *Int. J. Electron. Commun.*, vol. 53, pp. 305–314, 1999.

[2] V. Katkovnik and A. B. Gershman, "A local polynomial approximation based beamforming for source localization and tracking in nonstationary environments," in *IEEE Signal Processing Letter*, vol. 7, pp. 3–5, Jan. 2000.

[3] R. Schmidt, "Multiple emitter location and signal parameter estimation," *IEEE Transactions on Antennas and Propagation*, vol. 34, pp. 284–280, Mar. 1986.

[4] J. Reilly and S. Haykin, "Maximum likelihood receiver for low-angle tracking radar, parts I and II," *Proceedings of the Institute of Electrical Engineering*, vol. 129 Pt. F, pp. 261–272, 1982.

[5] M. Viberg and B. Ottersen, "Sensor array processing based on subspace fitting," *IEEE Transactions on Signal Processing*, vol. 39, pp. 1110–1121, May 1991.

[6] M. Wax and T. Kailath, "Detection of signals by information theoretic criteria," *IEEE Transactions on Acoustics, Speech and Signal Processing*, vol. 33, pp. 387–392, Apr. 1985.

[7] T. Kurien and R. Washburn, "Multiobject tracking using passive sensors," in *Proceedings of the American Control Conference*, (Boston, MA), 1985.

[8] C. Jauffret and Y. Bar-Shalom, "Track formation with bearing and frequency measurements in clutter," *IEEE Transactions on Aerospace and Electronic Systems*, vol. 26, pp. 999–1010, Nov. 1990.

[9] K. Pattipati, S. Deb, Y. Bar-Shalom, and R. Washburn, "A new relaxation algorithm and passive sensor data association," *IEEE Transactions on Automatic Control*, vol. 37, pp. 198–213, Feb. 1992.

[10] C. S. C. Rao and B. Zhou, "Tracking the direction of arrival of multiple moving targets," *IEEE Transactions on Signal Processing*, vol. 42, pp. 1133–1144, May 1994.

[11] B. Anderson and J. Moore, *Optimal Filtering*. Englewood Cliffs: Prentice-Hall, 1979.

[12] D. Aspach and H. Sorenson, "Nonlinear bayesian estimation using gaussian sum approximations," *IEEE Trans. Auto. Cont.*, vol. 17, no. 4, pp. 439–448, 1972.

[13] R. Bucy and K. Senne, "Digital sysnthesis of nonlinear filters," *Automatica*, vol. 7, pp. 287–298, 1971.

[14] Y. Bar-Shalom, X. R. Li, and T. Kirubarajan, *Estimation with Appliations to Tracking and Navigation*. New York: John Wiley & Sons, Inc., 2001.

[15] D. Johnson, "The application of spectral estimation to bearing estimation problem," *Proceedings of the IEEE*, vol. 70, pp. 1018–1028, Sept. 1982.

[16] D. Johnson and D. Dudgeon, *Array Signal Processing: Concepts and Techniques*. New Jersey: PTR Prentice Hall, 1993.

[17] T. Wigren and A. Eriksson, "Accuracy aspects of doa and angular velocity estimation in sensor array processing," in *IEEE Signal Processing Letter*, vol. 38, pp. 60–62, Apr. 1995.

[18] B. Yang, "An extension of the PASTd algorithm to both rank and subspace tracking.," *IEEE Signal Processing Letters*, vol. 2, pp. 179–182, Sept. 1995.

[19] C. Andrieu, N. D. Freitas, and A. Doucet, "Sequential MCMC for Bayesian model selection," in *Proceedings of the Internationl Workshop on Higher Order Statistics*, (Ceasarea, Israel), 1999.

[20] C. Andrieu, A. Doucet, W. Fitzgerald, and S. Godsill, "An introduction to the theory and applications of simulation based computational methods in Bayesian signal processing," in *Tutorial from Proceedings of the International Conference on Acoustics, Speech, and Signal Processing*, (Seattle, WA), 1998.

[21] N. Gordon, D. Salmond, and A. Smith, "Novel approach to non-linear/non-Gaussian Bayesian state estimation," *IEE Proceedings-F*, vol. 140, no. 2, pp. 107–113, 1993.

[22] A. Doucet, "On sequential simulation-based methods for Bayesian filtering.," Tech. Rep. TR.310, University of Cambridge, Department of Engineering, Signal Processing Group, England, 1998.

[23] P. Green, "Reversible jump Markov Chain Monte Carlo computation and Bayesian model determination," in *Biometrika*, vol. 82, pp. 711–732, 1995.

[24] S. Haykin, *Adaptive Filter Theory, 4th Edition*. Englewood Cliffs, NJ: Prentice Hall, 2000.

[25] C. Andrieu and A. Doucet, "Joint Bayesian model selection and estimation of noisy sinusoids via reversible jump MCMC," *IEEE Transactions on Signal Processing*, vol. 47, pp. 2667–2676, Oct. 1999.

[26] J.-R. Larocque, J. P. Reilly, and W. Ng, "Particle filter for tracking an unknown number of sources," *IEEE Transactions on Signal Processing*, vol. 50, pp. 2926–2937, Dec. 2002.

[27] W. Gilks, S. Richardson, and D. Spiegelhalter, *Markov Chain Monte Carlo in Practice*. New York: Chapman and Hall, 1998.

[28] A. Doucet, S. Godsill, and C. Andrieu, "On sequential Monte Carlo sampling methods for Bayesian filtering," *Statistics and Computing*, vol. 10, pp. 197–208, 2000.

[29] W. Hastings, "Monte Carlo sampling methods using Markov chains and their applications," in *Biometrika*, vol. 57, pp. 97–109, 1970.

[30] S. Godsill, "On the relationship between MCMC model uncertainty methods.," Tech. Rep. TR.305, Cambridge University, Engineering Department, England, Jan. 1998.

[31] C. Andrieu, *Méthodes MCMC pour l'analyse Bayesienne de modèles de régression paramétrique non-linéaire. Application à l'analyse de raies et à la déconvolution impulsionnelle.* PhD thesis, Université de Cergy-Pontoise, France, 1997.

[32] P. Troughton and S. Godsill, "Bayesian model selection for time series using Markov Chain Monte Carlo.," in *Proceedings of the IEEE International Conference on Acoustics, Speech, and Signal Processing*, (Munich, Germany), Apr. 1997.

[33] P. Troughton and S. Godsill, "A reversible jump sampler for autoregressive time series," in *Proceedings of the IEEE International Conference on Acoustics, Speech, and Signal Processing*, (Seattle, WA), Apr. 1998.